

Calibration of scintillation detectors for MeV charged fusion products

M. Tuszewski

Los Alamos National Laboratory, Los Alamos, New Mexico 87545

S. J. Zweben

Princeton Plasma Physics Laboratory, Princeton, New Jersey 08544

(Presented on 16 March 1992)

The light output of ZnS scintillators used to detect escaping fusion products in the TFTR Tokamak is studied with 3.5-MeV alpha and 3-MeV proton beams. The emitted light first increases linearly with beam current and then saturates. In all cases investigated, the saturations start at a fairly constant absorbed power density of about 1 mW/cm^2 . The scintillators have adequate time response up to 50–100 kHz.

I. INTRODUCTION

Scintillation detectors are used in the TFTR Tokamak to detect escaping charged fusion products.¹ Triton and proton fluxes of 10^8 – $10^9 \text{ cm}^{-2} \text{ s}^{-1}$ are measured on the scintillators in D-D experiments and alpha fluxes of 10^{10} – $10^{11} \text{ cm}^{-2} \text{ s}^{-1}$ are expected in D-T experiments. So far, only ZnS(Ag) has been used, but ZnS(Cu) is considered for future experiments.² The light output of these scintillators has been studied in some detail³ at fluxes of about $10^3 \text{ cm}^{-2} \text{ s}^{-1}$. Further work at higher fluxes is required for quantitative information from this diagnostic. Specific issues to be investigated are light output linearity, radiation damage, efficiency at high temperatures, and time response in the frequency range 0–1 MHz. In this paper, we report results obtained with a Curium alpha source and with Van de Graaf ion beams that address some of the above issues.

II. EXPERIMENTAL APPARATUS

The scintillators are studied at the Los Alamos Ion Beam Facility in a vacuum chamber sketched in Fig. 1. A ZnS powder of average thickness $9 \pm 1 \mu\text{m}$ is deposited on a 2.5×2.5 -cm quartz substrate. The scintillator is fixed in an aluminum holder mounted on a stem that can be remotely moved up or down or rotated at any angle φ with respect to the ion beam direction. Measurements with the ^{244}Cm source are made by placing the source 1 cm in front of the scintillator (rotated at $\varphi = 180^\circ$) and by monitoring the emitted light through the quartz substrate. The Van de Graaf experiments are made with the ion beam entering from the left side on Fig. 1 through vertical and horizontal apertures. These apertures define small rectangular cross sections that are fully intercepted by the scintillator. For all experiments reported here, φ was set at 20° to simulate TFTR experimental cases.¹ Before and after each measurement, the scintillator is lowered to determine the beam current with a large area Faraday cup shown in Fig. 1.

The emitted light is collected by a train of three lenses that image the scintillator onto the photocathode of a photomultiplier tube (Hamamatsu R-762) with a magnification of 0.7. The PM tube is surrounded by a magnetic shield case and by a light-tight container. The output of the PM tube is connected to a preamplifier (Thorn EMI A1-101). The amplified anode current is measured on a stor-

age oscilloscope (Tektronix 2330) with a $50\text{-}\Omega$ termination. The vacuum chamber has negligible stray light and is pumped down to 10^{-6} Torr. An observation port indicated in Fig. 1 is used to check the beam position on the scintillator with a video camera.

III. CURIUM SOURCE RESULTS

The light emitted by the scintillator has been assumed to be proportional to the energy deposited into the phosphor by the charged particles.¹ This assumption is tested by inserting aluminum foils of thickness δ between the Curium source and a P-11 ZnS(Ag) scintillator. The relative light output measured as function of δ is indicated with solid circles in Fig. 2. A simple calculation of the energy deposited into the scintillator is also shown with a solid line in Fig. 2. The calculation assumes that the alpha energy distribution is a Gaussian of 3.7-MeV central energy and of 1.4-MeV (FWHM) width. This distribution is an approximate fit to measurements made with a surface barrier diode. The model shows reasonable agreement with the data in Fig. 2. Presumably, an even better agreement could be obtained by including opacity³ and angular scattering effects. A maximum in light output is obtained for $\delta = 1.5 \mu\text{m}$ rather than for $\delta = 0$ because the mean alpha range somewhat exceeds the average scintillator thickness

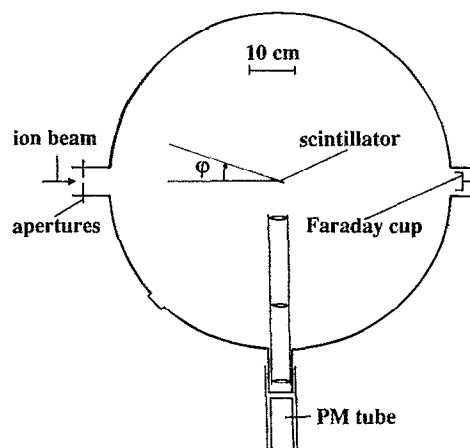


FIG. 1. Sketch of the experimental apparatus.

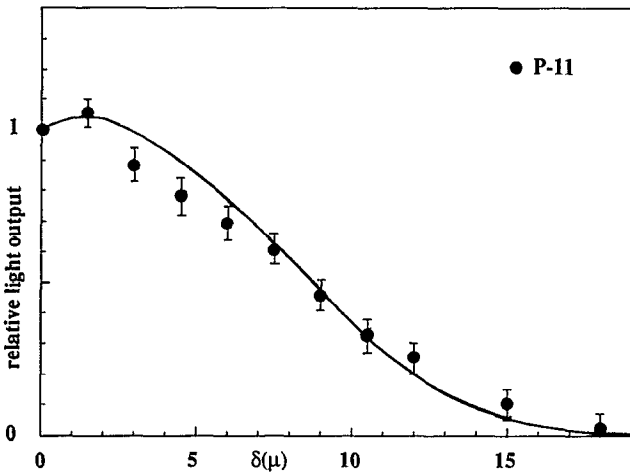


FIG. 2. Relative light output as function of the aluminum foil thickness placed in front of the Curium source.

viewed from the source. The results in Fig. 2 suggest that the emitted light is indeed approximately proportional to the energy deposited into the ZnS phosphor.

The linearity of the scintillator light output as function of the alpha particle flux is studied by varying the distance between the Curium source and the scintillator. For each distance in the range 0.2–8 cm, the alpha flux is computed from the measured source activity of $2.2 \times 10^7 \text{ s}^{-1}$ and from the solid angle to the scintillator boundary. The light output (arbitrary units) is shown with solid circles in Fig. 3 as function of the alpha flux. These data are obtained with a PM tube voltage of 0.5 kV, a preamplifier termination of 1 M Ω , and a blue filter (Corion P70-450-S) in front of the photocathode. The arbitrary straight line in Fig. 3 suggests that the emitted light is proportional to the alpha flux in the range 10^4 – $10^6 \text{ cm}^{-2} \text{ s}^{-1}$.

IV. VAN DE GRAAF RESULTS

A. Beam current dependence

The P-11 ZnS(Ag) and the P-31 ZnS(Cu) scintillators are studied with 3.5-MeV alphas and 3-MeV protons

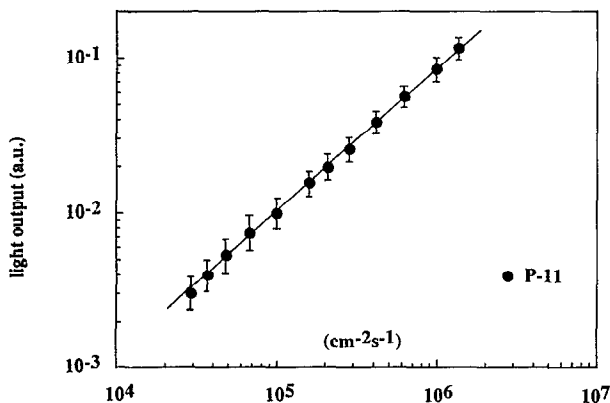


FIG. 3. Light output as function of the alpha particle flux from the Curium source.

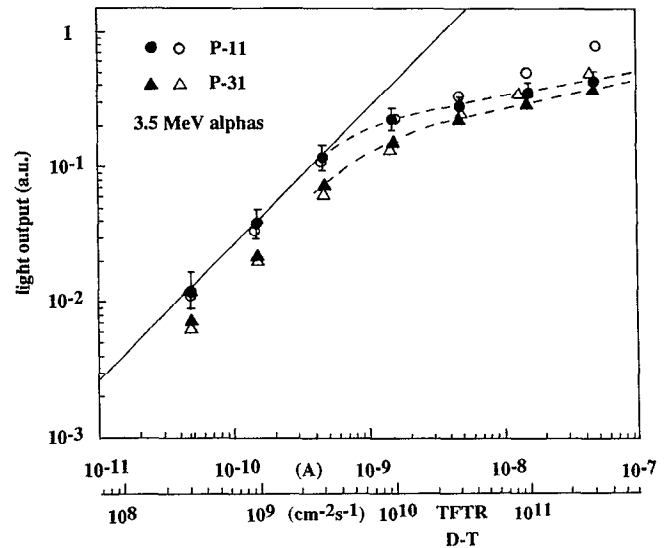


FIG. 4. Light output as function of beam current for 3.5-MeV alphas. The dotted lines outline departures from linearity. The solid and hollow symbols are for steady and chopped beams, respectively.

beams in the range 10^{-11} – 10^{-7} A. The light outputs (arbitrary units) are shown as functions of beam current in Figs. 4 and 5. The corresponding particle fluxes are also indicated. These data are obtained with a PM tube voltage of 0.2 kV, a preamplifier termination of 1 M Ω , and apertures 0.4 by 0.4 cm that yield an area A of about 0.5 cm² on the scintillators oriented at $\varphi=20^\circ$. The hollow symbols correspond to chopped (10 ms on, 90 ms off) beams.

The scintillator light output first increases linearly with beam current and then saturates in Figs. 4 and 5. Similar saturations with ZnS(Ag) have been noted with 10–30 keV electrons beams,⁴ with onsets at power densities of a few mW/cm². The onset of the saturations in Figs. 4 and 5

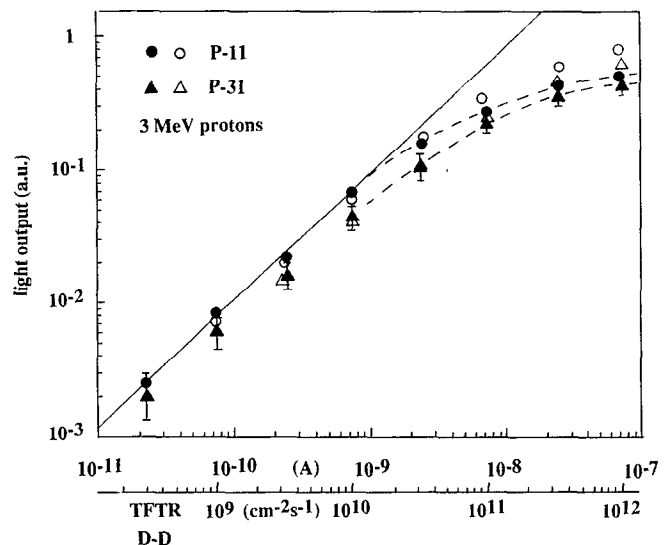


FIG. 5. Light output as function of beam current for 3-MeV protons. The dotted curves outline departures from linearity. The solid and hollow symbols are for steady and chopped beams, respectively.

correspond to absorbed power densities $\Delta EI_c / ZeA$ of 1.4 mW/cm², where ΔE (3.5 MeV for alphas and 0.8 MeV for protons) is the energy deposited within the ZnS powder, Z is the atomic number, and I_c (0.4 nA for alphas and 0.9 nA for protons) is the onset current. The cause of the saturations remains unclear. Aside from possible instrumental problems, the main potential causes are (1) radiation damage, (2) heating of the scintillator, (3) charge accumulation, and (4) saturation of the luminescent centers.

Radiation damage contributes somewhat to the saturations, as can be seen by comparing data with steady and chopped beams in Figs. 4 and 5. The scintillators are exposed for 60–100 s at each current, resulting in final fluences of $(2-3) \times 10^{13}$ cm⁻² for steady beams and of $(2-3) \times 10^{12}$ cm⁻² for chopped beams in Fig. 4. The scintillating efficiencies decrease permanently by about 20% after 3×10^{12} α /cm² and by 60–70% after 3×10^{13} α /cm², in rough agreement with previous results.² Scintillator heating does not appear to contribute much to the observed saturations. The temperature of the back of the scintillator was monitored with a thermocouple and did not increase by more than 50 °C at the highest current levels. In addition, energy estimates suggest that the ZnS temperature could not increase by more than 10–20 °C at the onset of the saturations. Charge accumulation at the surface and within the scintillator may contribute substantially to the observed saturations.⁴ The video recordings show a gradual transition from well-defined to diffuse impacted areas as the current is increased. Occasional sparks are observed at high currents. Various tests are under way to explore the influence of charge build-up. Saturation of the luminescent centers may also contribute to the observed saturations.

For a given flux within the linear current ranges, the emitted light is about five times larger for alphas in Fig. 4 than for protons in Fig. 5. However, this factor is mostly accounted for by the difference in ΔE . For given conditions, P-31 yields about half as much light as P-11, but most of this factor comes from the reduced PM tube efficiency (60%) in the green relative to the blue.

B. Time response

A slow chopper, already introduced in the context of Figs. 4 and 5, shows that both P-11 and P-31 have excellent time responses in the range 0–1 kHz. A fast chopper is used to extend these studies up to 1 MHz. Current pulses of 1- μ s duration and with rise and decay times of a few ns are produced at selected time intervals. An example with 12.8- μ s period is shown in Fig. 6(a) from a fast Faraday cup. The responses of the P-11 and P-31 scintillators to this current waveform are shown in Figs. 6(b) and 6(c), respectively. These traces are obtained with a peak proton current of 0.75 nA and with the lowest preamplifier gain which yields a 20-ns rise time. Both responses are qualitatively similar, with a relatively fast rise and a slower decay. The rise and decay consist of a fast initial component and a subsequent slower component consistent with fluorescence and phosphorescence processes.⁴ The slow decay times limit the resolution at high frequencies. One can crudely attribute a single exponential decay time to each

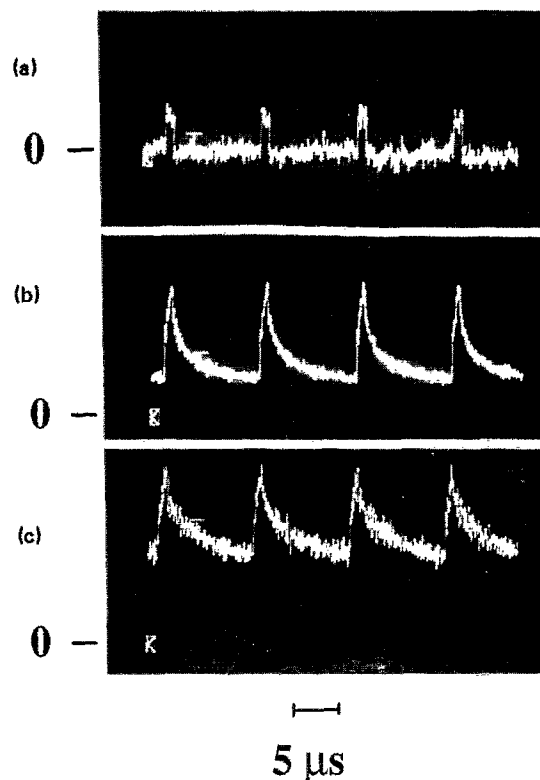


FIG. 6. Voltage traces showing (a) a chopped 3-MeV proton beam current, (b) the response of the P-11 scintillator, and (c) the response of the P-31 scintillator.

scintillator by considering the ratios of maximum to minimum signals in Figs. 6(b) and 6(c). One obtains 9 μ s for P-11 and 18 μ s for P-31. These decay times do not change appreciably at 75 pA and at 7.5 nA. Hence, the P-11 and P-31 scintillators can resolve oscillations of frequency less than 100 and 50 kHz, respectively. This is adequate for most but not all instability-induced oscillations (0–1 MHz) that may be present in Tokamak discharges.²

ACKNOWLEDGMENTS

The authors are indebted to Rita Gribble, Dick Scarborough, and to the staff of the Los Alamos Ion Beam Facility for excellent technical assistance. This work was supported by the U.S. DOE.

¹S. J. Zweben, R. L. Boivin, C. S. Chang, G. W. Hammett, and H. E. Mynick, *Nucl. Fusion* **31**, 2219 (1991).

²S. J. Zweben, R. Boivin, S. L. Liew, D. K. Owens, J. D. Strachan, and M. Ulrickson, *Rev. Sci. Instrum.* **61**, 3505 (1990).

³R. L. Boivin, Ph.D. thesis, Princeton Plasma Physics Laboratory Report PPPL-2797 (1991).

⁴V. L. Levshin *et al.*, in "Soviet Researches on Luminescence", *Transactions of the Lebedev Physics Institute*, edited by Acad. D. V. Skobel'tsyn, Consultants Bureau Enterprises, Inc., NY (1964), Vol. 23.